ELSEVIER

Analytica Chimica Acta 318 (1995) 125–136

ANALYTICA CHIMICA ACTA

# Corrections for heteroscedasticity in window evolving factor analysis

Christian Ritter, Jean A. Gilliard *, Jean Cumps, Bernard Tilquin

*School of Pharmacy, Université Catholique de Louvain, Avenue Mounier 72, B-1200 Brussels, Belgium*

Received 28 April 1995; revised 14 July 1995; accepted 28 August 1995

**Abstract**

Window evolving factor analysis (WEFA) is a powerful technique for checking peak purity in liquid chromatography with diode array detection (LC-DAD). However, practical application of the technique can be limited by instrumental and experimental non-idealities. One of the problem sources is heteroscedasticity. In this work, we propose two new data transformation procedures and one technique for directly adjusting the log-eigenvalue profiles, which eliminate most of the heteroscedastic effect in the WEFA plots. The pretreatment and the adjustment techniques can be used in combination to obtain even better results. The performance of the techniques are demonstrated on simulated and actual data.

*Keywords:* Liquid chromatography; Heteroscedasticity; Factor analysis; Chemometrics; Window evolving factor analysis

## 1. Introduction

Assurance of the purity of drugs is of utmost importance in pharmaceutical practice. One commonly used technique for impurity detection is liquid chromatography (LC) coupled with a UV–visible diode array detector (DAD). The data set generated by a LC-DAD system is called a spectrochromatogram and can be described in matrix form in which the rows are the absorption spectra measured at regular time intervals and the columns are the chromatograms measured at different wavelengths. Various mathematical treatments of spectrochromatograms to assess chromatographic peak purity have been proposed [1–10].

Window evolving factor analysis (WEFA) is a relatively recent and powerful technique for checking peak purity in LC-DAD. It has been developed independently in several laboratories and was referred to as fixed size window evolving factor analysis [1], differential evolving factor analysis [11] or window evolving factor analysis [3]. The technique is commercially implemented in the Beckman Gold DAD software [12]. In WEFA, one performs a series of principal components analyses on a moving subset of the original data matrix containing a fixed number of spectra. Each successive window of spectra is reduced to a set of eigenvalues whose logarithms are plotted as a function of elution time. The number of eigenvalues is equal to the number of spectra in the window. When the chromatogram is on the baseline, all the eigenvalues are of about the same magnitude and small. When a single component peak elutes,

* Corresponding author.


*SSDI* 0003-2670(95)00434-3

one eigenvalue grows large while the others remain small and of about the same size. In the case of a two components peak, two eigenvalues will rise above the rest, and so on.

WEFA permits a sensitive peak purity assessment without the need for a reference of known purity and gives complementary information such as the number of solutes coeluting under the investigated peak and where coelutions occur [1–3].

However, when applying WEFA one has to be aware of some practical limitations. Several instrumental and experimental non-idealities can cause the number of eigenvalues emerging from the noise level to exceed the number of underlying chemical species and lead therefore to false alarms in purity control [13,14]. Possible sources of such artefacts include a non-zero or sloping baseline, the DAD scan time, a non linear response and heteroscedasticity. These factors have been studied in some details by Keller and co-workers [14–16], and mathematical corrections have been proposed for non-zero or sloping baseline [14], scan time [15] and heteroscedasticity [16].

In this work, alternative corrections for the effect of heteroscedastic noise in WEFA are proposed.

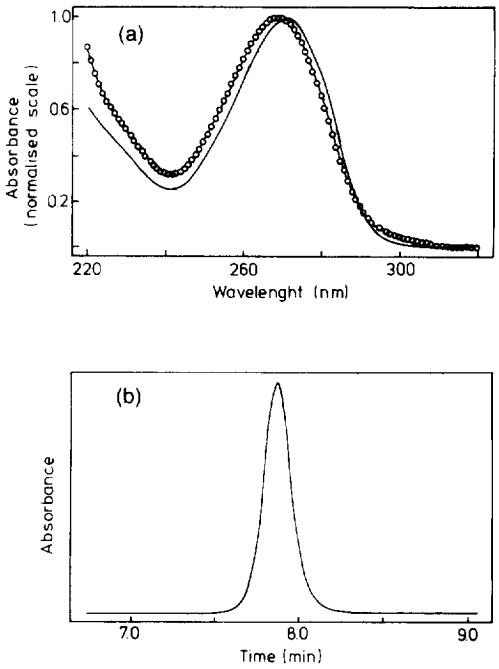


Fig. 1. (a) Normalised spectra of theophylline (—) and paraxanthine (---) measured in the presence of an acetonitrile–water (15:85, v/v) mobile phase; (b) actual chromatographic profile used in simulation.

## 2. Experimental

### 2.1. Chemicals

The samples consisted of theophylline (Fluka, Buchs, Switzerland) dissolved in the mobile phase. Their concentration was adjusted to give a maximum absorbance in the range from 0.1 to 0.7 AU at 271 nm ($\lambda_{max}$ in the spectral range investigated). The mobile phase consisted of 15% acetonitrile (LC grade, Labscan, Dublin, Ireland) in water (obtained from an in-house water purification system, Milli-Q, Millipore, Milford, MA). To quantify heteroscedasticity, the data were collected at stopped flow. The flow rate was otherwise 1 ml/min.

### 2.2. Instruments

The LC system consisted of a Beckman dual pump Model 126 (Beckman, Fullerton, CA) and a Rheodyne injection valve Model 7725i with a 20 $\mu$l sample loop (Rheodyne, Cotati, CA). A 250 × 4 mm i.d. RP-18 column (Merck, Lichrospher RP-select B, 5 $\mu$m) was used at ambient temperature. The DAD system was a Beckman Model 168 equipped with a fixed 4 nm optical slit and was operated in the 'resolution mode', with a scan rate of 32 Hz. The spectra were collected with a sampling rate of 4 Hz, covering the wavelength range from 220 to 320 nm with a resolution of 1 nm. After collection, the data were converted to ASCII files using the Beckman ArrayView software.

### 2.3. Simulation

The experimentally recorded spectra of two isomeric compounds, theophylline and paraxanthine, used in the simulation are shown in Fig. 1a. The main analyte was theophylline while the impurity was paraxanthine. The same actual peak shape was used in the simulation of the spectrochromatograms of both the main component and the impurity (Fig. 1b) and simulated impure data sets were obtained by

superimposing the spectrochromatograms with a variable chromatographic resolution defined as $R_s = 2\Delta t/(W_a + W_b)$ where $\Delta t$ represents the distance between chromatographic maxima and $W_a$ and $W_b$ are the respective widths of the bases of the peaks. Proportional heteroscedastic noise was superimposed to the noise-free simulated spectrochromatogram by the following relation:

$$s_{ij} = s_0(1 + \alpha y_{ij})\xi_{ij} \quad (1)$$

where $s_{ij}$ is the standard deviation of the noise at time $i$ and wavelength $j$, $s_0$ is the standard deviation of the baseline noise, $y_{ij}$ is the signal measured at time $i$ and wavelength $j$, $\alpha$ is a proportionality factor, and $\xi_{ij}$ is a standard normal random number.

If $\alpha$ is equal zero, homoscedastic data are simulated. An $\alpha$ value of 7 was found to provide good agreement between simulated and actual heteroscedastic data (see below).

Simulation and data analysis were performed using routines written in-house in the Windows version of S-PLUS (Statistical Sciences, Seattle, WA). All calculations were done on a Pentium based IBM-compatible personal computer.

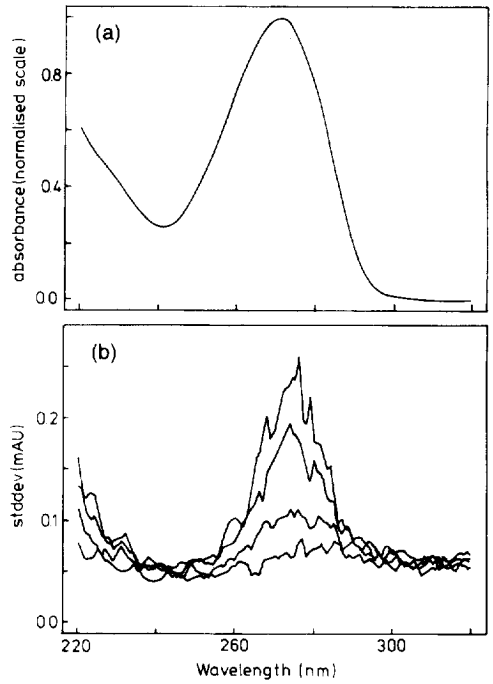


Fig. 2. (a) normalised spectra of theophylline; (b) standard deviation of eighty consecutively measured spectra with a maximal absorbance of respectively 0.1, 0.3, 0.5 and 0.7 AU.

## 3. Non idealities in LC-DAD data

### 3.1. Heteroscedasticity

Heteroscedastic noise or a measurement variance which changes with the magnitude of the signal is not uncommon in analytical chemistry [17]. In UV–visible spectroscopy, it is logical that the noise increases with absorbance since increased absorbance is related to decreased light throughput.

To demonstrate the presence of heteroscedasticity and to assess its importance, several solutions with increasing concentrations of theophylline ($A_{max}$ of respectively 0.1 to 0.7 AU) were measured with DAD at stopped flow. Each time, eighty spectra were recorded consecutively and the standard deviation of the absorbances was computed for each wavelength. This standard deviation can be interpreted as the noise level and is plotted against wavelength in Fig. 2b. Clearly, the noise is distinctly heteroscedastic when absorbance becomes relatively large, and follows the shape of the absorbance spectrum. Fig. 3 shows that the relationship between the noise and the signal is approximately linear with an intercept around $4 \times 10^{-5}$ AU and a slope around $28 \times 10^{-5}$. The intercept can be interpreted as baseline noise and the slope as the degree of heteroscedasticity. This gives rise to the model for noise simulation given in Eq. (1) with $s_0 = 4 \times 10^{-5}$ and $\alpha = 7$. This model was used to simulate spectrochromatograms in order to show the effect of het-

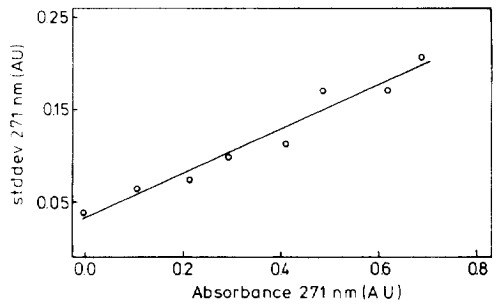


Fig. 3. Standard deviation (stddev) versus wavelength plot for the data collected at stopped flow for several peak absorbances.

eroscedasticity on WEFA profiles without the interference of other non idealities.

Fig. 4 shows the WEFA plots for the first five eigenvalues (EVs) obtained for simulated pure and impure (0.5% impurity, $R_s = 0.5$) homoscedastic peaks and for the corresponding pure and impure heteroscedastic peaks ($\alpha = 7$). The window size (wz) used for the WEFA was equal to the full width at half maximum of the investigated peak, i.e., 10 spectra [18]. For a pure peak, the first EV accounts for the sole chemical species under the peak and its logarithm shows typically a taper-shaped profile, whereas the higher order EVs summarise noise. Under homoscedasticity, the higher order EVs remain small and show flat log-profiles throughout the elution time (Fig. 4a). Any second bulge in the WEFA plot would therefore be attributed to an impurity as in Fig. 4b. However, under heteroscedasticity, the increased noise level associated with the chromatographic elution profile causes the higher order log EV traces to bulge out locally, even for a pure peak (Fig. 4c). If any deviation in the log EV profiles is interpreted as the presence of an impurity, this leads to false alarms. If one considers only detachments of the lower order log EV profiles from the higher order ones as sign of impurity, the interpretation is still more complicated than in the homoscedastic situation (Fig. 4d).

### 3.2. Other sources of non-idealities

In practice at absorbance levels where heteroscedastic noise can be clearly observed, other non-ideality sources, particularly deviations from linearity due to polychromatic radiation and stray light, are of greater concern [19]. Bertolin [20] has pointed out that the linearity of diode array detectors is more limited than that of a photomultiplier spectrophotometer due to the use of a wider wavelength band-pass to optimise the signal to noise ratio. Dose and Guiochon [21] derived non-linear equations which describe the dependence of the DAD response on the bandpass and on the shape of the absorption spectrum of the sample. Gerritsen et al. [13] have shown

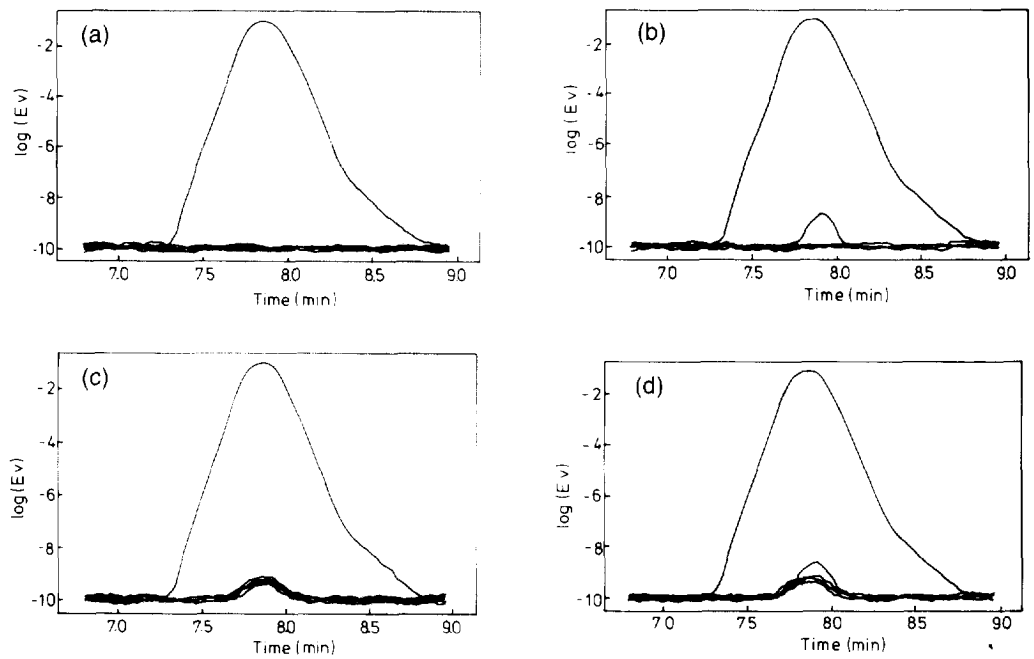


Fig. 4. WEFA plots (limited to the first 5 EVs, wz = 10) obtained for several simulated peaks (maximal absorbance of 0.4 AU and baseline noise $s_0$ of $4 \times 10^{-5}$ AU): (a) pure homoscedastic peak, (b) impure (0.5% impurity, $R_s = 0.5$) homoscedastic peak, (c) pure peak with superimposed heteroscedastic noise according to Eq. (1) ($\alpha = 7$), (d) impure heteroscedastic peak (0.5% impurity, $R_s = 0.5$).

that the examination of the shape of the eigenvectors calculated by singular value decomposition of the spectrochromatogram, can reveal the presence of such non-linearities in the data. With our DAD, which is equipped with a fixed 4 nm optical slit, the response can be distinctly non-linear at absorbances as low as 0.2 AU under normal chromatographic conditions. Fig. 5 shows the structure of the first six eigenvectors (score vectors) computed for an actual homogeneous peak of theophylline (Fig. 5a) and for simulated homoscedastic and heteroscedastic data sets (Fig. 5b and c), all with a maximum absorbance

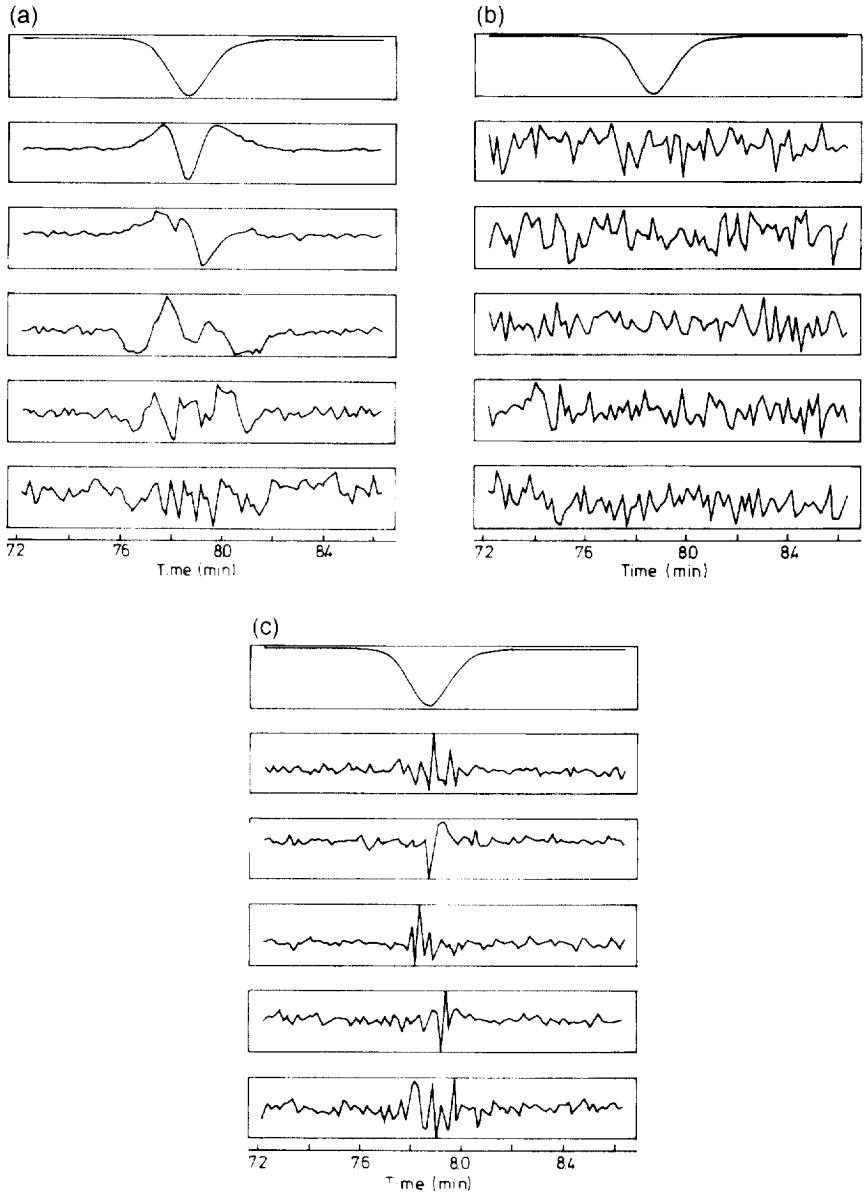


Fig. 5. Structure of the first to the sixth eigenvector of (a) an actual pure theophylline peak, (b) a simulated pure homoscedastic peak, (c) a simulated pure peak with added heteroscedastic noise according to Eq. (1) ($\alpha$ = 7); all with an $A_{max}$ of 0.2 AU.

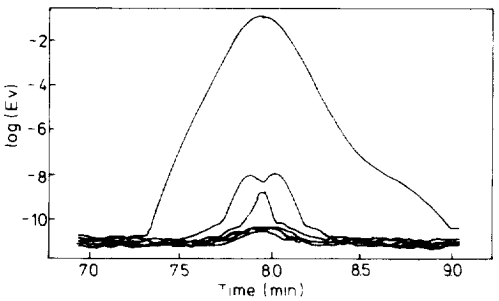


Fig. 6. WEFA plots (limited to the first 6 EVs, wz = 10) obtained for an actual pure peak with an $A_{max}$ of 0.5 AU.

of 0.2 AU. From this picture we can see that in contrast with what is expected for the eigenvector structure of pure bilinear data, the second to the sixth eigenvectors of the real data contain more that only noise information. These eigenvector structures show large similarities with those observed by Gerritsen et al. with homogeneous anthracene solutions and various DAD systems [13]. In simulation, pure heteroscedasticity leads to eigenvectors representing noise with increased intensity under the region of higher absorbance of the peak. Although heteroscedasticity affects all eigenvectors, such a structure is only clearly apparent for the sixth eigenvector computed for the actual data, indicating that other sources of non linearity effectively dominate.

Fig. 6 shows the WEFA plot limited to the first six log EV profiles, obtained for a measured pure peak of theophylline peak with a maximum absorbance at about 0.5 AU. It demonstrates the combined effect of heteroscedasticity and other sources of non-idealities. The second and third eigenvectors are clearly associated with the non-linearity sources, whereas the bulge observed in the higher order log EV traces is related to heteroscedastic pattern.

## 4. Corrections for heteroscedasticity

Corrections for heteroscedastic noise are aimed at fully or partially reverting the situations shown in Fig. 4c and d into situations displayed in Fig. 4a and b. In particular, this means that a correction for heteroscedasticity should not destroy other structures of the data. A classical approach consists in transformation to approximate homoscedasticity prior to data analysis [16,22]. As we have shown the noise standard deviation of LC-DAD data displays a linear dependence on the signal. This suggests converting to logarithms. However, the logarithmic transformation is inappropriate since it destroys the bilinear structure of the data. In the following, alternative procedures for the correction of heteroscedasticity in WEFA are proposed.

### *4.1. Adjusting the raw data by spectral standardisation*

#### *4.1.1. Method 1*

Appropriate pretreatment procedures for transformation of LC-DAD data to reduce heteroscedasticity may take advantage of the proportional relationship observed between the noise and the signal. The transformation proposed by Keller et al. [16] belongs to this category. In this procedure, each spectrum is divided by its sum, provided that the latter exceeds a predefined threshold $z$:

$$y_{t\lambda}^{*} = y_{t\lambda}\left(\sum_{i=1}^{n} y_{ti}\right)^{-1} \text{ if } \sum_{i=1}^{n} y_{ti} \geq z \tag{2}$$

and

$$y_{t\lambda}^{*} = y_{t\lambda} \text{ if } \sum_{i=1}^{n} y_{ti} < z \tag{3}$$

where $y_{t\lambda}$ is the signal measured at time $t$ and wavelength $\lambda$, $n$ is the number of wavelengths and $y_{t\lambda}^{*}$ is the corrected signal. A threshold is imposed in order to avoid noise inflation at small absorbance values.

#### *4.1.2. Method 2*

Here we proposed the alternative following transformation:

$$y_{t\lambda}^{*} = y_{t\lambda}\left(1 + \bar{y}_t \beta\right)^{-1} \tag{4}$$

where $\bar{y}_t$ is the mean value of the spectrum measured at time $t$ and $\beta$ is a proportionality factor. The choice of the denominator is designed to produce a smooth transition from the part of the spectrochromatogram at baseline to the part containing the peak so that the correction does not require thresholding. The transformation will perform best if $\beta$ is chosen close to the actual noise proportionality factor $\alpha$.

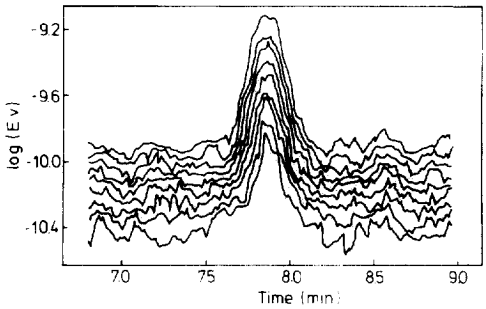


Fig. 7. Second to the tenth log EV profiles obtained for the WEFA of the data from Fig. 4c.

#### 4.1.3. Method 3

A second possibility, which makes no explicit assumption about the relationship between the noise and the signal, is to correct all signals $y_{t\lambda}$ of a spectrum by a local estimation of the noise $s_t$:

$$y^*_{t\lambda} = y_{t\lambda}/s_t \tag{5}$$

This can be done in various ways. We suggest smoothing each spectrum by a simple running median, to retain the residuals and to estimate $s_t$ from the latter. As discussed in the following section, this

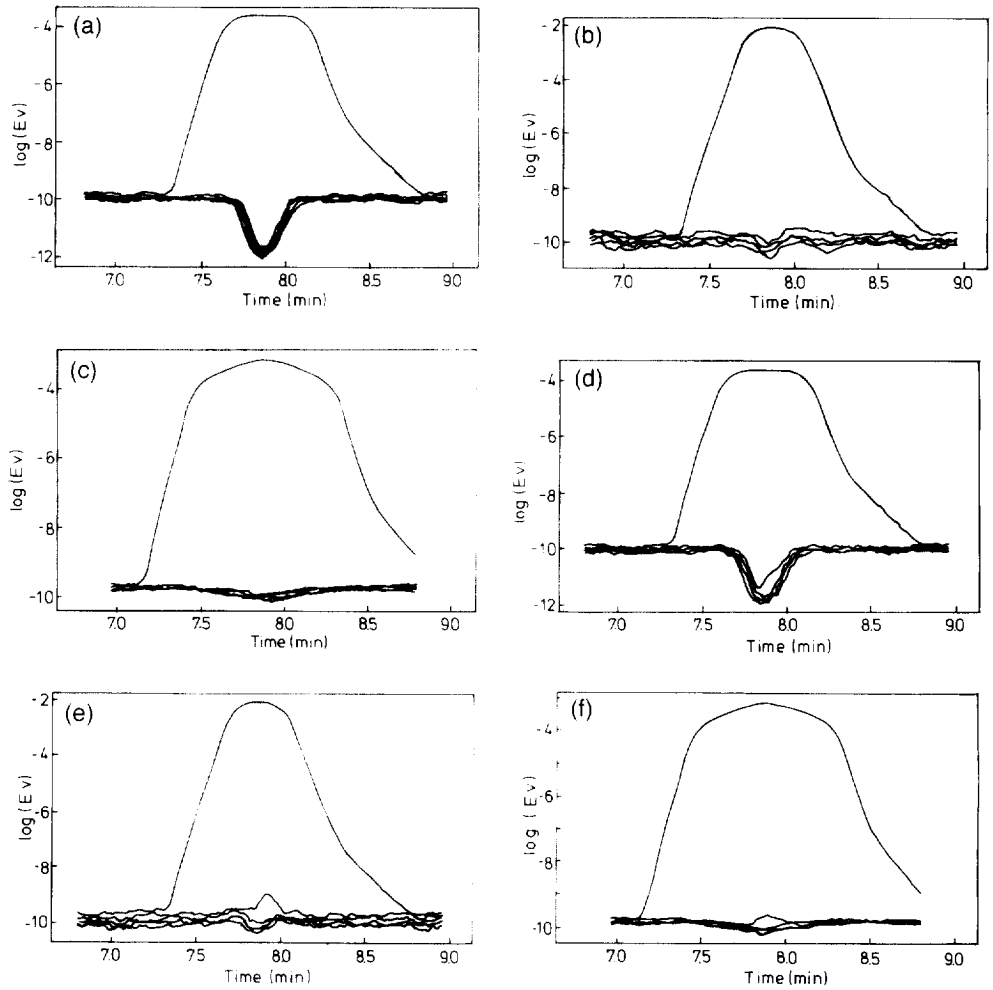


Fig. 8. WEFA plots (limited to the first 5 EVs) obtained with correction procedure according to Eq. (2) and (3) with $z = 1$, for the data of Fig. 4c (pure heteroscedastic peak): (a) spectral resolution = 1 nm, 25 spectra treated and wz = 10, (b) spectral resolution = 5 nm, 14 spectra treated and wz = 10, (c) same as in (a) except for wz = 30; (d to f) idem for the data of Fig. 4d (impure heteroscedastic peak).

should be done by a robust estimator such as the median of the absolute residuals.

#### 4.1.4. Adjusting the log EV profiles: Method 4

Finally, an alternative strategy to data pre-processing can be imagined. Fig. 7 shows the second to the tenth log EV profiles observed for the data from Fig. 4c (pure heteroscedastic peak). We note that these profiles remain approximately parallel showing that heteroscedasticity affects all the EVs summarising the noise. This can be exploited in the following way. If we assume that only the $p$ first EVs are sufficient to summarise all the relevant information in the spectrochromatogram, the higher order EVs will summarise the noise and can be used to measure the effect of heteroscedasticity. Therefore, a correction can be obtained by subtracting the $p+1$st log EV trace from the lower order ones. However as high order log EV profiles express the noise and are hence rough, using them directly leads to inflated noise in the corrected profiles. Therefore, it is better to smooth the higher order trace before adjustment. A simple smoothing method such as running medians or averages suffices.

## 5. Results and discussion

### 5.1. Method 1

Fig. 8 shows the result of applying the first correction procedure Eqs. (2) and (3) to the data displayed in Fig. 4c and d. A value of 1 was arbitrarily chosen for the threshold $z$. Since the correcting factor is the sum of the corresponding spectrum, the performance of the technique will depend heavily on the spectral resolution used for data collection. In our examples, if a 1 nm resolution is used, the correcting factor is too large and the noise level in the central region of the peak where the treatment is applied (i.e., the part of the peak where the sum of the spectrum is larger than $z$) is much smaller than towards the edges of the peak where the data are not corrected. Consequently, the log EV profiles display a clear negative distortion in the region where the spectra were corrected (Fig. 8a and d). In our situation, if the spectral resolution is changed to 5 nm more satisfactory results are observed (Fig. 8b and e). The negative distortion in the log EV profiles can also be attenuated by using a

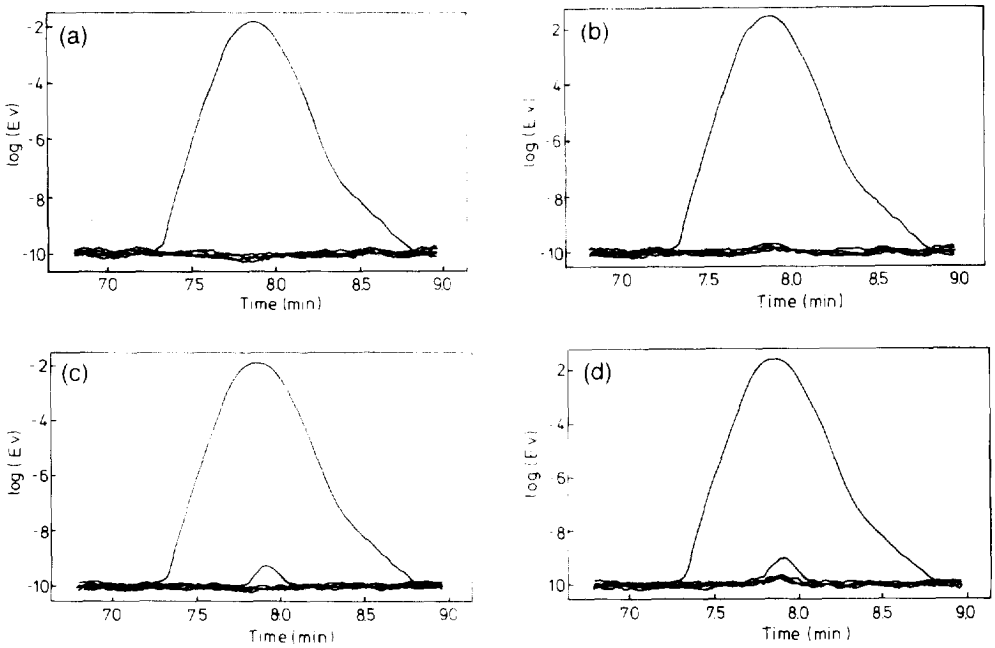


Fig. 9. WEFA plots (limited to the first 5 EVs, wz = 10) obtained with correction procedure according to Eq. (4) for the data of Fig. 4c (pure heteroscedastic peak): (a) $\beta = 10$, (b) $\beta = 5$; (c and d) idem for the data of Fig. 4d (impure heteroscedastic peak).

moving window which includes a number of spectra larger than the number of spectra corrected (Fig. 8c and f). In this case, the distortion becomes more moderate, since the noise level in each moving window overlapping with the peak lies between the baseline noise and the corrected noise. A too large window will however lower the sensitivity of the analysis (see Fig. 8f) and increase the computation time [18].

### 5.2. Method 2

The problems affecting the first method are associated with thresholding and resolution-dependent adjustment. These can be avoided if, first, a resolution-independent summary of the spectrum such as the mean, is used as correcting factor instead of the sum. Secondly, the correction can be constructed without the need of a threshold. Those ideas are the basis of Eq. (4): the form of its denominator implies that the noise level at baseline remains practically unchanged while providing a correction similar to Method 1 in the high part of the peak. The required proportionality factor $\beta$ should be taken close to the actual heteroscedasticity factor $\alpha$. It depends on the instrument characteristics and can be estimated using the approach described earlier. Fig. 9 shows the result of applying the correction procedure according to Eq. (4) to the data displayed in Fig. 4c and d, with $\beta$ values of 10 (Fig. 9a and c) and of 5 (Fig. 9b and d). The optimal value for $\beta$ being equal to $\alpha$, i.e., 7. From this picture, we can see that the technique performs well and is relatively insensitive to an inaccurate estimation of $\beta$ (30–40% of error).

In Fig. 10a we see that most of the heteroscedasticity-induced bulge in the log EV profiles of the actual data set of Fig. 6, can effectively be removed by applying the correction procedure according to relation (4) with an estimated $\beta = \alpha = 7$ (Fig. 9b).

### 5.3. Method 3

Whereas Method 2 still requires estimation of $\beta$, Method 3, i.e., the correction according to Eq. (5), is appealing because it requires neither an assumption about the relationship between the noise and the

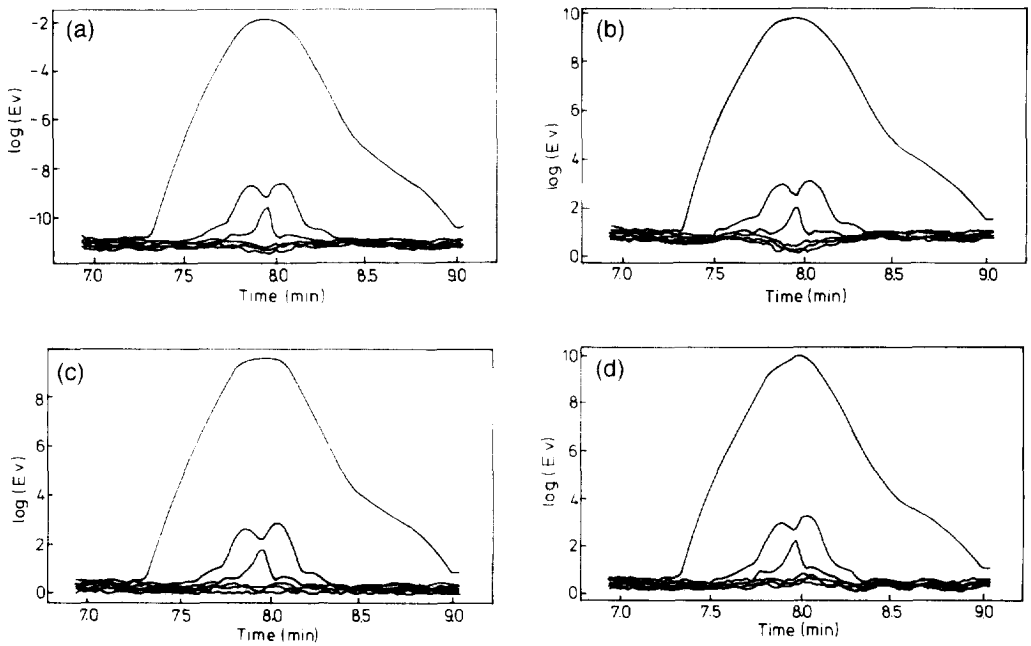


Fig. 10. WEFA plots (limited to the first 6 EVs, wz = 10) obtained for the actual data of Fig. 6 (a) by applying correction procedure according to Eq. (4), (b) by applying correction procedure according to Eq. (5), (c) by subtracting the sixth log EV profiles, (d) by combining correction according to Eq. (5) and the subtraction of the tenth log EV profile.

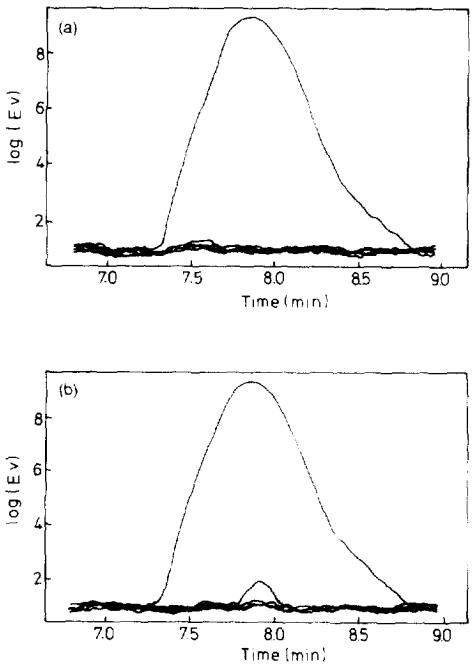


Fig. 11. WEFA plots (limited to the first 5 EVs, wz = 10) obtained with correction procedure according to Eq. (5) for the data of (a) Fig. 4c (pure heteroscedastic peak), and (b) Fig. 4d (impure heteroscedastic peak).

signal, nor an a priori estimation of a multiplication factor. Fig. 11 displays the result of applying Method 3 to the data displayed in Fig. 4c and d, showing that this techniques performs well for pure heteroscedastic data. In practice however, other sources of non-ideality can lead to an overestimation of the data variability even if a robust estimator is used (median of the absolute residuals rather than their standard deviation). This is illustrated in Fig. 10b for the application of this transformation technique to actual data: a slight negative distortion can now be observed in the profiles of the third to the sixth log EV indicating that the correction is too strong.

### 5.4. Method 4

Alternatively to data transformation procedures such as described above, the effect of heteroscedasticity in WEFA can be corrected by subtracting a high order log EV profile from the lower order ones. The reasoning behind this strategy is that all relevant information is contained in the lower order EVs whereas the higher order ones express only noise. As for Method 3, such a correction procedure does not

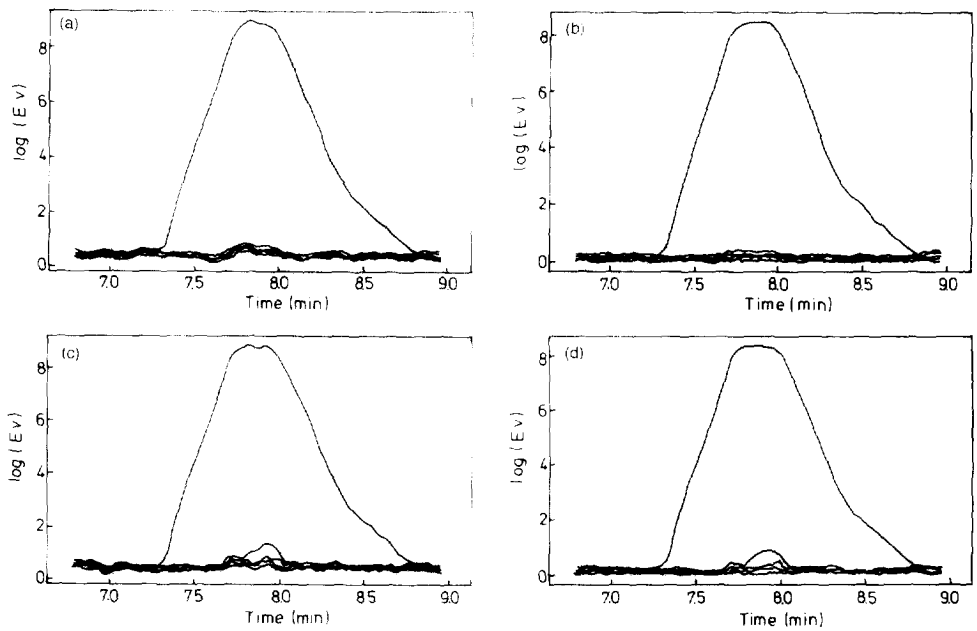


Fig. 12. WEFA plots (limited to the first 5 EVs, wz = 10) obtained by adjusting the log EV profiles for the data of Fig. 4c (pure heteroscedastic peak): (a) subtraction of the sixth trace, (b) subtraction of the tenth trace; (c and d) idem for the data of Fig. 4d (impure heteroscedastic peak).

require an explicit assumption about the relationship between noise and signal. However, it will perform best if the noise is proportional to the signal since in this case, the increased absolute noise in the peak region results in a positive and parallel shift of all log EV traces. Fig. 12 shows the result of the application of this technique to the simulated data from Fig. 4c and d, for the subtraction of respectively the last log EV trace (i.e., the tenth; Fig. 12a and c) and the sixth (Fig. 12b and d). Due to the subtraction, the coordinate scale is now shifted in the positive values, the baseline level corresponding approximately to zero. In practice, since heteroscedasticity does not affect all the eigenvectors summarising the noise exactly simultaneously (see Fig. 7), better result are expected when the order of the subtracted log EV profile is close to the order of the traces from which it is subtracted (compare Fig. 12a and b). Satisfactory results were obtained by subtracting the sixth log EV profile. Fig. 10c shows the result obtained for the subtraction of the sixth trace in the case of the actual data set. Of course, we must then assume that the number of chemical species coeluting under a region of the investigated peak corresponding to the width of the moving window, will not exceed five. Under normal chromatographic conditions, such an assumption may be regarded as reasonable for most applications.

The applicability of the trace subtraction method will also depend on the size of the window used in WEFA. If the window is very small, only few EVs can be computed and there are not sufficiently many higher order EVs available to allow a reliable estimation of the heteroscedasticity correction. However, such small window sizes are of limited interest since sensitivity is low compared to windows which are as wide as the full width at half maximum of the investigated peak [18]. Considering that 15–20 data points have to be collected across a chromatographic peak in order to avoid distortion in the peak shape and to guarantee accurate retention time and peak area calculations [23], effective windows contain therefore at least 7 spectra and make the method applicable.

### 5.5. Methods combination

Higher order log EV trace subtraction can also be applied after data transformation in order to improve an incomplete correction due to an imperfect estimation of the proportionality factor in Eq. (4) or an overestimation of the noise according to Eq. (5). The pretreatment tends to make log EV profiles more parallel and permits subtracting higher order traces than without prior data transformation. For instance, the subtraction of the tenth traces allows to correct the slight negative deviations induced by the application of the transformation according to relation (5) to the actual data set (compare Fig. 10b and d). In this case, room is left for up to nine compounds coeluting under the span of the moving window.

## 6. Conclusion

Although WEFA is a very powerful technique for peak purity assessment in LC-DAD, its practical application is limited by instrumental and experimental non-idealities. One of the problem sources is heteroscedasticity. Two possible strategies for correction for non-uniform variance are the transformation to homoscedasticity prior to WEFA and the direct elimination of the effect of heteroscedasticity on the log EV traces.

Based on the first strategy, two new data pretreatment techniques are proposed. The first one relies on the observed linear relationship between noise and intensity of the LC-DAD data, as the method developed by Keller and co-workers. However, in contrast with their technique, our procedure is independent on the digital resolution of the spectra and does not require the specification of a threshold for its application. Nevertheless, a proportionality factor has to be experimentally estimated.

Our second transformation technique proposed relies on a local estimation of the noise and has hence the advantage of avoiding the estimation of a multiplier constant.

Finally, most of the heteroscedastic effect can also be eliminated by simply subtracting a log EV profile accounting for heteroscedasticity from the lower order log EV profiles.

Whereas the three proposed techniques perform equally well with simulated data, better results were obtained for the trace subtraction procedure when working with actual data. The application of this correction technique however requires that non relevant eigenvalues are available for the adjustment

computation. If the window is very small, a data preprocessing method will be the only viable choice.

## References

[1] H.R. Keller and D.L. Massart, Anal. Chim. Acta, 246 (1991) 379.
[2] H.R. Keller, D.L. Massart and J.O. De Beer, Anal. Chem. 65 (1993) 471.
[3] H.R. Keller, P. Kiechle, F. Erni, D.L. Massart and J.L. Excoffier, J. Chromatogr., 641 (1993) 1.
[4] Y.-z. Liang, O.M. Kvalheim, H.R. Keller, D.L. Masart, P. Kiechle and F. Erni, Anal. Chem., 64 (1992) 946.
[5] S.J. Vanslyke and P.D. Wentzell, Chemom. Intell. Lab. Syst., 20 (1993) 183.
[6] F.C. Sanchez, M.S. Khots and D.L. Massart, Anal. Chim. Acta, 285 (1994) 181.
[7] F.C. Sanchez, M.S. Khots and D.L. Massart, Anal. Chim. Acta, 290 (1994) 249.
[8] F.C. Sanchez and D.L. Massart, Anal. Chim. Acta, 298 (1994) 331.
[9] G.A. Bakken and J.H. Kalivas, Anal. Chim. Acta., 300 (1995) 173.
[10] J.B. Casteldine and A.F. Fell, J. Pharm. Biomed. Anal., 11 (1993) 1.
[11] J. Kankare, J. Lukkari, T. Pajunen, J. Ahonen and C. Visby, J. Electroanal. Chem. Interfacial Electrochem., 294 (1990) 59.
[12] J. Schaefer, Int. Chromatogr. Lab., 1 (1990) 6.
[13] M.J.P. Gerritsen, N.M. Faber, M. van Rijn, B.G.M. Vandeginste and G. Kateman, Chemom. Intell. Lab. Syst., 12 (1992) 257.
[14] H.R. Keller and D.L. Massart, Anal. Chim. Acta, 263 (1992) 21.
[15] H.R. Keller, D.L. Massart, P. Kiechle and F. Erni, Anal. Chim. Acta, 256 (1992) 125.
[16] H.R. Keller, D.L. Massart, Y.-z. Liang and O.M. Kvalheim, Anal. Chim. Acta, 263 (1992) 29.
[17] J.S. Garden, D.G. Mitchell and W.N. Mills, Anal. Chem., 52 (1980) 2310.
[18] J.A. Gilliard, C. Ritter, J. Cumps and B. Tilquin, Anal. Chim. Acta., submitted for publication.
[19] H.J.P. Sievert and A.C.J.H. Drouen, in L. Hubert and S.A. George, Diode Array Detection in LC, Marcel Dekker, New York, 1993, pp. 72–73.
[20] M. Bertolin, Int. Lab., October (1991) 44.
[21] E.V. Dose and G. Guiochon, Anal. Chem., 61 (1989) 2571.
[22] O.M. Kvalheim, F. Brakstad and Y.-z. Liang, Anal. Chem., 66 (1994) 43.
[23] G.I. Ouchi, LC-GC Int., 10 (1991) 18.